35th Annual International Conference of the IEEE EMBS
Osaka, Japan, 3 - 7 July, 2013

EEG Classification of Physiological Conditions in 2D/3D Environments Using Neural Network*

Wajid Mumtaz, *Member, IEEE,* Likun Xia, *Member, IEEE,* Aamir Saeed Malik, *Senior Member, IEEE,* Mohd Azhar Mohd Yasin

***Abstract*—Higher classification accuracy is more desirable for brain computer interface (BCI) applications. The accuracy can be achieved by appropriate selection of relevant features. In this paper a new scheme is proposed based on six different nonlinear features. These features include Sample entropy (*SampEn*), Composite permutation entropy index (*CPEI*), Approximate entropy (*ApEn*), Fractal dimension (*FD*), Hurst exponent (*H*) and Hjorth parameters (complexity and mobility). These features are decision variables for classification of physiological conditions: Eyes Open (*EO*), Eyes Closed (*EC*), Game Playing 2D (*GP2D*), Game playing 3D active (*GP3DA*) and Game playing 3D passive (*GP3DP*). Results show that the scheme can successfully classify the conditions with an accuracy of 88.9%.**

I. Introduction

In past, automated procedures based on nonlinear neural signal processing techniques for electroencephalogram (EEG) signals were not used. Correct interpretations were mainly based on expert opinions. There might be human errors involved in observations and interpretations. Recent advances in nonlinear signal processing techniques for EEG have shown promise in this direction, and commonly known as quantitative EEG (QEEG). Features extracted through QEEG methods can be used as decision variables for classification of physiological conditions.

EEG signals are considered non-stationary, therefore nonlinear feature extraction methods are employed for information extraction. For example nonlinear feature extraction and application of neural networks can be helpful to automate the diagnosis of epilepsy. Features like entropies [1] [2], fractal dimension [3] and Hurst exponent [4] were used for classification of normal and seizure conditions in humans [5]. Moreover same authors also employed frequency domain features such as wavelet coefficients and higher order spectral (HOS) components. Various classifiers had been used as well, such as spiking neural network [6], back propagation neural network [7], radial basis function neural network [8] , multi-spiking neural network [9], recurrent neural network [10], support vector machine [11], fuzzy [12] and to name a few. Some other examples are the studies of changes in brain dynamics during playing games in 2D/3D environments have been conducted recently [13, 14].

In this paper we have tested six features: sample entropy (*SampEn*) [1], approximate entropy (*ApEn*) [1], composite permutation entropy index (*CPEI*) [2], fractal dimension (*FD*) [3] , hurst exponent (*H*) [4] hjorth complexity [15]. EEG data were captured during five physiological conditions: eyes close (*EC*), eyes open (*EO*), game playing in 2D (*GP2D*) and 3D (*GP3DA*, *GP3DP*) environments. The proposed scheme is based on features extraction and their arrangements into a feature space. In addition, a neural network was trained to classify the physiological conditions. Neural Network Pattern Recognition (NNPR) toolbox was used [16].

Structure of the paper is described. Section II consists of mathematical description of nonlinear EEG features. Section III describes data acquisition and analysis. Section IV explains classification performance: confusion matrix and receiver operating characteristics (ROC). Section V concludes the paper.

II. Feature Extraction

A. Sample Entropy

Considering EEG as time series, *SampEn* can be used to compute complexity. An algorithm developed by Richman and Moorman described below [1].

a) Formulate m dimension vectors consecutively from the EEG time series, starting with the i^{th} point described in (1).

$$X(i) = [x(i), x(i+1), \ldots, x(i+m-1)] \quad (1)$$

Where $i, j = 1, 2, \ldots, N-m+1, j \neq i$.

b) Distances of vectors are computed for every i^{th} value as in (2)

$$d[X(i), X(j)] = \max_{k=0,1,\ldots m-1} [|x(i+k) - x(j+k)|] \quad (2)$$

c) Given a tolerance window r, count the number of this distance, which is less than or equal to r, denoted as $B_i(r)$. Then calculate the ratio of this number to $N-m-1$, indicated in (3).

$$B_i^m(r) = \frac{1}{N-m-1} B_i \quad (3)$$

d) Calculate average value of $B_i^m(r)$

*Resrach supported by Ministry of Higher Education Malaysia.

Mr. Wajid Mumtaz is with the Centre for Intelligent Signal and Imaging (CISIR), Universiti Teknologi PETRONAS, Tronoh 31750, Malaysia (phone: +60 111 525 4260; e-mail: wajidmumtaz@gmail.com).

Dr. Likun Xia and Dr. Aamir Saeed Malik are with Centre for Intelligent Signal and Imaging (CISIR), Universiti Teknologi PETRONAS, Tronoh 31750, Malaysia (e-mail: likun_xia@petronas.com.my).

Mr. Mohd Azhar Mohd Yasin is affiliated with Department of Psychiatry, Universiti Sain Malaysia (e-mail: mdazhar@kb.usm.my).

$$B^m(r) = \frac{1}{N-m+1}\sum_{i=1}^{N-m+1} B_i^m(r) \quad (4)$$

e) Increase the dimension to *m+1*, and repeat steps from a) to d) to calculate $B_r^{m+1}(r)$

$$B^{m+1}(r) = \frac{1}{N-m+1}\sum_{i=1}^{N-m+1} B_i^{m+1}(r) \quad (5)$$

$$SampEn(m,r,N) = -\ln[\frac{B^{m+1}(r)}{B^m(r)}] \quad (6)$$

To compute *SampEn*, a run length *m*, and a tolerance window *r* are required. Generally *m=1*, and *r= 0.2SD*. *SD* is the standard deviation of the original data i.e., *X(i)*.

B. Approximate Entropy

ApEn is used for a measurement of complexity of time series. A time series with N data points can be written as $\{x(n) = x(1), x(2), ..., x(N)\}$.

a) Formulate *N-M+1* vectors *X(1)....X(N-M+1)* defined in (7). Where *i=1,...,N-m+1*.

$$X(i) = [x(i), x(i+1), ..., x(i+m-1)] \quad (7)$$

b) Find distance between *X(i)* and *X(j)* as: (8).

$$d[X(i), X(j)] = \max_{k=1,2,..,m} |x(i+k-1) - x(j+k-1)| \quad (8)$$

c) For a given *X(i),* count the number of *j (j=1...N-m+1)* fulfilling condition *d[X(i), X(j)]* ≤ *r*, and is denoted as $N^m(i)$. '*r*' is tolerance value and *i=1...N-m+1*.

$$C_r^m(i) = N^m(i)/(N-m+1) \quad (9)$$

$C_r^m(i)$ measures frequency of similar patterns within window length *m*.

d) Compute the natural logarithm of each $C_r^m(i)$ and average it over '*i*'.

$$\phi^m(r) = \frac{1}{N-m+1}\sum_{i=1}^{N-m+1} \ln C_r^m(i) \quad (10)$$

e) Increase in dimension by one i.e., *m+1*. Repeat previous steps to find $C_r^{m+1}(i)$ and $\phi^{m+1}(r)$.

$$ApEn(m,r,N) = \phi^m(r) - \phi^{m+1}(r) \quad (11)$$

The parameters '*m*', '*r*' and '*N*' are similar as in case of *SampEn*.

C. Composite Permutation Entropy Index

CPEI is a nonlinear method and reflects complexity of time series. It can be achieved described below [2].

a) The continuous EEG signal is fragmented into a sequence of motifs. Motifs are shapes of six different types as in Figure 1. These shapes can explain most of the changes in an EEG signal.

b) Identification of each motif similar to one of the possible six types.

c) To obtain probability of occurrence of each motif count number of motifs of each type in the signal.

d) Shannon uncertainty formula is used to calculate permutation entropy (*PE*). It is based on normalized probability distribution of the motifs.

For calculation of *CPEI*, two *PEs* with different parameters; noise threshold and lag are added. Mathematically it is described as (12).

$$CPEI = \frac{\sum p_i \times \ln(p_i)_{,tie<0.5,\tau=1} + \sum p_i \times \ln(p_i)_{,tie<0.5,\tau=2}}{\ln(49)} \quad (12)$$

Where noise threshold (tie<0.5 uV) and lag (τ) may be equal to either 1 or 2. To obtain correct normalization in denominator of (12), six motifs from P_τ and one from PE_{ties} are used to make a total of 49 (7x7).

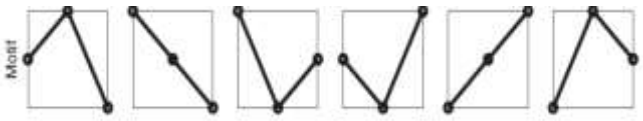

Figure 1. Motifs

D. Fractal Dimension

Considering EEG as time series, fractal dimension D_f computes complexity and irregularity. It ranges from D_f=*1* for a simple curve to D_f=*2* for a curve which nearly fills out a whole plan. The algorithm constructs *k* new time series for a given time series: *X(1), X(2),.....,X(N),* described in (13).

$$X_m^k : X(m), ..., X(m + \text{int}((N-m)/k) \times k) \quad (13)$$

Where *m=1,2,...,k* and *N* is total number of samples, *k* is interval time, *m* is initial time, *int(r)* is integer part of a real number *r*. (14) presents mathematical formula for length $L_m(k)$, of each curve X_m^k :

$$L_m(k) = \frac{1}{k}\left|\sum_{i=1}^{M} |X(m+i\times k) - X(m+(i-1)\times k)|\right|\left(\frac{N-1}{M\times k}\right) \quad (14)$$

Curve length, *L(k)*, for time interval *k*, is calculated as mean of the *k* values i.e., $L_m(k)$ where *m= 1, 2,..., k* as described in (15).

$$L(k) = \left(\frac{\sum_{m=1}^{k} L_m(k)}{k}\right) \quad (15)$$

The value of fractal dimension D_f is calculated by a least-square linear best-fitting procedure. It is equivalent to the slop coefficient of the linear regression of the *log/log* graph of $L(k) = k^{-D_f}$.

E. Hurst Exponent

H is used to evaluate correlation properties and self-similarities of fractional Brownian noise; a time series prsoduced by a fractional Gaussian process. It is described by (16).

$$H = \log(R/S)/\log(T) \tag{16}$$

In (17) the statistic "*R/S*" can be calculated.

$$\frac{R(T)}{S(T)} = \frac{(\max(X(t,T)) - \min(X(t,T)))}{\sqrt{\frac{1}{T}\sum_{t=1}^{t}(x(t)-\bar{x})^2}} \tag{17}$$

A graph is plotted among two quantities i.e., *ln(R(n)/S(n))* and *ln(n)*. *H* is slop of the graph. '*T'* is sample data time duration. Corresponding value of rescaled range is '*R/S'*.

F. Hjorth Complexity and Mobility

Activity, mobility and complexity were defined by Hjorth as a set of parameters for quantitative description of an EEG while considering EEG signal as time series [15]. Activity can be computed as variance of signal, a_0 as: (18). Mobility can be calculated as variance of slope of the EEG, a_2. It is normalized by variance of the amplitude distribution of time series as: (19). Complexity is calculated as variance of rate of slope changes, a_4 with reference to an ideal sine curve described by (20). Hjorth complexity was employed for simulation purposes.

$$Activity : A = a_0 \tag{18}$$

$$Mobility : M = [a_2/a_0]^{1/2} \tag{19}$$

$$Complexity : C = [a_4/a_0]^{1/2} \tag{20}$$

III. METHODOLOGY

A. Data Acquisition

Experiment design for EEG data acquisition is described. A total of twenty nine (29) participants were recruited. After initial screening and signing of consent forms, participant was asked to sit on a chair in a quiet room with dim lights. A wearable 24 electrodes EEG cap was used, 19 electrodes were used for EEG data acquisition, 3 for ECG and 2 for reference. ECG was not recorded for this study.

Software named *BrainMaster Discovery* was used for data acquisition, pre-processing. Sampling rate was 256 Hz, band pass filter was 0.5-70 Hz and an additional 50 Hz notch filter for power line noise filtration. Data were amplified by an amplifier named *Brain Master 24E*.

EEG data acquisition was performed during *EC*, *EO* and game playing on 2D and 3D screens. In 3D, the same game was played in two different conditions; 3D active (*GP3DA*) and 3D passive (*GP3DP*). Active and passive conditions were created by using active and passive 3D glasses. Passive 3D glasses were the normal cinema glasses whereas active glasses have a battery for automatic operation. Duration for *EO* and *EC* was 5 minutes each, and 3 minutes for game playing conditions.

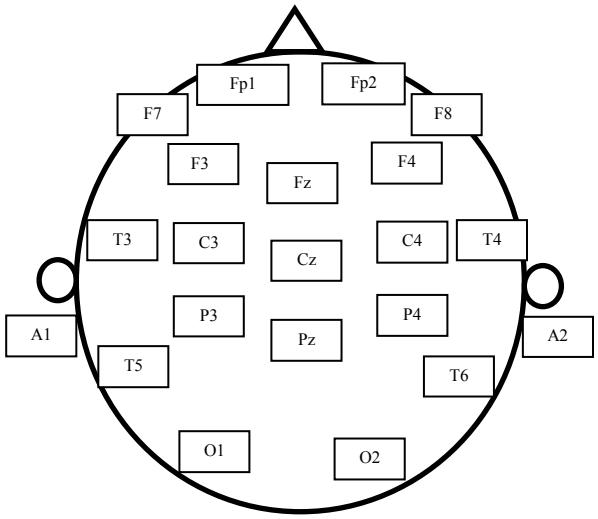

Figure 2. Topographical Electrode Locations

B. Data Analysis

For computation reduction, scalp electrodes were grouped according to their locations to represent five brain regions as explained. Frontal region consists of electrodes Fp1, Fp2, F7, F3, Fz, F4 and F8. Central region includes electrodes Cz, C3 and C4. Temporal region consists of electrodes T3, T4, T5, and T6. Parietal and occipital regions comprise electrodes Pz, P3, P4 and O1, O2, respectively. The topographic map showing 19 electrode locations are described by Figure 2.

The individual six features were computed for 19 electrodes during the five physiological conditions. To reduce the computational time and to represent a single brain region averaging was carried out. Since there were five brain regions and each region had 6 feature values for each condition, therefore 30 different values were computed for each brain region. A feature space matrix with size 29×150 consists of 150 samples (five physiological conditions × six features × five brain regions; 5×6×5) was formulated.

Classification was performed by using NNPR. Feature space was divided into three subsets; training, validation and test samples. Both training and validation samples were used to train the classifier. We used 7 participants' data as test data and rest of the participant's data as training (25% test data, 75% training). Number of neurons in hidden layers was 20. A two layer neural network was employed. The stopping criterion was *validation stop*. Learning rate was set to 0.01, and momentum constant was 0.9.

IV. RESULTS

Figure 3 is a confusion matrix; a visual description of accuracy of the proposed scheme. It is representing number of correct and incorrect classifications for the test samples. Each condition: *EC*, *EO*, *GP2D*, *GP3DA*, *GP3DP* is considered as a class and is specified by numbers 1, 2, 3, 4 and 5 respectively. Rows represent target/actual classes whereas columns represent output/predicted classes. Among

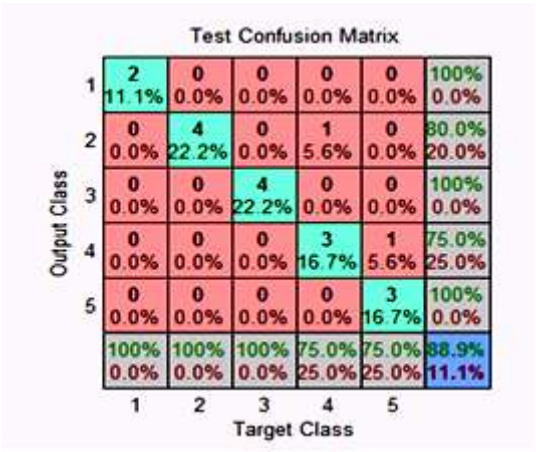

Figure 3. Confusion Matrix

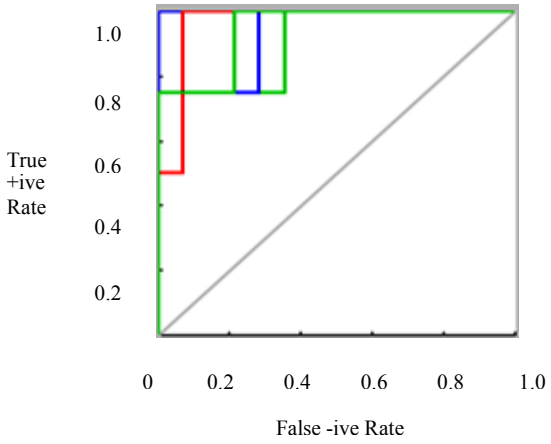

Figure 4. ROC Graph

eighteen (18) test samples, the output classes *EC*, *EO* and *GP2D* were classified with 100% accuracy. The *GP3DA* and *GP3DP* were classified with 75% accuracy. This can be seen across the diagonal of the confusion matrix. The overall classification accuracy was 88.9% for all conditions.

Figure 4 shows ROC analysis results for the test samples, and provides accuracy of the proposed scheme. The center line in the ROC graph represents 50% accuracy. An approximation named 'One class vs. all other classes' was adapted to plot multiclass ROC graph. A good classifier should have its values in the upper left side corner. Physiological conditions: *EC*, *EO* and *GP2D* with 100% classification were in the upper left corner of the graph, whereas *GP3DA* and *GP3DP* showed some deflections.

V. Conclusion

This paper proposed a new scheme based on unique feature set for classification of physiological conditions using resting state and 2D, 3D games data. Five brain regions were analyzed. The results showed that these features can be used in classification of these physiological conditions with a reasonable accuracy. This scheme has a potential to be used in the automation of diagnosing diseases. Following these findings, in future different classifiers will be employed to observe that which one may provide even better classification results for the same set of features.

Acknowledgment

This work is supported by Fundamental Research Grant Scheme (Ref: FRGS/1/2012/TK02/UTP/03/03), Ministry of High Education (MOHE), and URIF (Ref: URIF 12/2012), Universiti Teknologi PETRONAS, Malaysia.

References

[1] S. L. Richman and J. R. Moorman, "Physiological time series analysis using approximate entropy and sample entropy," *Am. J. Physiol. Heart Physio,* vol. 278, pp. H2039-H2049, 2000.

[2] L. Xiaoli, S. Cui, and L. J. Voss, "Using permutation entropy to measure the electroencephalographic effects of Sevoflurane," *Anesthesiology,* vol. 109, pp. 448-456, 2008.

[3] A. Accardo, M. Affinito, M. Carrozzi, and F. Bouquet, "Use of the fractal dimension for the analysis of electroencephalographic time series," *Biol. Cybern.,* vol. 77, pp. 339-350, 1997.

[4] K. Natarajan, R. A. U, F. Alias, T. Tiboleng, and S. K. Puthusserypady, "Nonlinear analysis of EEG signals at different mental states," *BioMedical Engineering OnLine,* pp. 3-7, 2004.

[5] U. R. Acharya, S. V. Sree, and J. S. Suri, "Application of non-linear and wavelet based features for the automated identification of epileptic eeg signals," *International Journal of Neural Systems,* vol. 22, pp. 125002 1-14, 2012.

[6] S. Ghosh-Dastidar and H. Adeli, "Improved spiking neural networks for EEG classification and epilepsy and seizure detection," *Integrated Computer-Aided Engineering,* vol. 14, pp. 187–212, 2007.

[7] S. Ghosh-Dastidar, H. Adeli, and N. Dadmehr, "Mixed-band wavelet-chaos-neural network methodology for epilepsy and epileptic seizure detection," *IEEE Transactions on Biomedical Engineering,* vol. 54, pp. 1545–1551, 2007.

[8] S. Ghosh-Dastidar, H. Adeli, and N. Dadmehr, "Principal component analysis enhanced cosine radial basis function neural network for robust epilepsy and seizure detection," *IEEE Transactions On Biomedical Engineering,* vol. 55, pp. 512–518, 2008.

[9] S. Ghosh-Dastidar and H. Adeli, "A new supervised learning algorithm for multiple spiking neural networks with application in epilepsy and seizure detection," *Neural Networks,* vol. 22, pp. 1419–1431, 2009.

[10] N. F. Guler, E. D. Ubey, and I. Guler, "Recurrent neural network employing Lyapunov exponents for EEG signals classification," *Expert Systems with Applications,* vol. 29, pp. 506-514, 2005.

[11] K. C. Chua, V. Chandran, U. R. Acharya, and C. M. Lim, "Automatic identification of epileptic EEG signals using higher order spectra," *International Journal of Engineering in Medicine,* vol. 223, pp. 485–495, 2009.

[12] U. R. Acharya, F. Molinari, V. S. Sree, S. Chattopadhyay, K. H. Ng, and J. S. Suri, "Automated diagnosis of epileptic EEG using entropies," *Biomedical Signal Processing and Control,* vol. 7, pp. 401-408, 2012.

[13] A. S. Malik, A. A. Pauzi, D. A. Osman, and R. N. H. R. Khairuddin, "Disparity in Brain Dynamics for Video Games Played on Small and Large Displays," presented at the 2012 IEEE Symposium on Humanities, Science and Engineering Research, 2012.

[14] A. S. Malik, D. A. Osman, A. A. Pauzi, and R. N. H. R. Khairuddin, "Investigating Brain Activation with respect to Playing Video Games on Large Screens," presented at the 4th International Conference on Intelligent and Advanced Systems: A Conference of World Engineering, Science and Technology Congress (ESTCON), Kuala Lumpur, 2012.

[15] B. Hjorth, "EEG analysis based on time domain properties," *Electroencephalogr Clin Neurophysiol,* vol. 29, pp. 306–310, 1970.

[16] H. Demuth, M. Beale, and M. Hagan, "Neural Network Toolbox User's Guide," ed USA: The MathWorks, Inc, 2009.